International Journal of Automotive Technology, Vol. 4, No. 1, pp. 47–55 (2003)

1229–9138/2003/011–06

TRADE-OFFS BETWEEN FUEL ECONOMY AND NOX EMISSIONS USING FUZZY LOGIC CONTROL WITH A HYBRID CVT CONFIGURATION

A. ROUSSEAU*, S. SAGLINI, M. JAKOV, D. GRAY and K. HARDY

Argonne National Laboratory 9700, South Cass Avenue, Building 362 – Rm. C265, Argonne, IL64439-4815, U.S.A.

(Received 19 October 2002)

ABSTRACT–The Center for Transportation Research at the Argonne National Laboratory (ANL) supports the DOE by evaluating advanced automotive technologies in a systems context. ANL has developed a unique set of compatible simulation tools and test equipment to perform an integrated systems analysis project from modeling through hardware testing and validation. This project utilized these capabilities to demonstrate the trade-off in fuel economy and Oxides of Nitrogen (NOx) emissions in a so-called 'pre-transmission' parallel hybrid powertrain. The powertrain configuration (in simulation and on the dynamometer) consists of a Compression Ignition Direct Ignition (CIDI) engine, a Continuously Variable Transmission (CVT) and an electric drive motor coupled to the CVT input shaft. The trade-off is studied in a simulated environment using PSAT© with different controllers (fuzzy logic and rule based) and engine models (neural network and steady state models developed from ANL data).

KEY WORDS : CVT, Fuzzy logic control strategy, Hybrid vehicle, NOx emission

1. INTRODUCTION

The search for improved fuel economy and reduced emissions, without sacrificing performance, safety, reliability, and affordability has made the hybrid vehicles a challenge for the automotive industry. Diesel engines offer high fuel economy, but produce undesirable emissions (particulate matter and NOx) in conventional vehicles. Hybridization, i.e., by adding a traction motor and energy storage, can potentially reduce these emissions by operating the engine in the optimum efficiency range and capturing regenerative braking during deceleration.

To better understand the potential benefits of hybridization, ANL has developed an integrated set of tools for modeling, simulating and testing propulsion components, systems and vehicles. The first phase of this study, described in this paper, demonstrates the fuel economy versus NOx emissions trade-off in simulation. The second phase, still in process, will attempt to demonstrate similar results in hardware using the Hardware-In-the-Loop (HIL) test cell at the APRF.

PSAT, developed under Matlab/Simulink, was used in this study because it is a forward-looking model, allowing realistic control strategies to be developed that can be translated directly for use with the hardware in the APRF. PSAT is a command-based model, meaning that vehicle performance is estimated from the calculated component torque response to realistic commands, such as throttle for the engine, displacement for the clutch, gear number for the transmission, or mechanical braking for the wheels. Essentially, a driver model attempts to follow a pre-defined speed cycle. Since the simulated components react realistically to the commands and transient effects are taken into account (such as engine starting, clutch engagement/disengagement, or shifting), realistic control strategies can be developed.

Several PSAT characteristics, previously described (Deville and Rousseau, 2001; Rousseau *et al.*, 2001), have been useful in the study:

(1) Flexibility to exchange control strategies while the rest of the powertrain model remains the same;

(2) Easily exchanged component models to facilitate the comparison of steady-state and neural network engine models;

(3) Capability to run batch mode;

(4) Validated component and vehicle models (Rousseau *et al.*, 2001).

The characteristics of the conventional (reference) and hybrid vehicles are listed in the following table and Figure 1 shows the PSAT Simulink model of the pre-

**Corresponding author*. e-mail: arousseau@anl.gov

Table 1. Comparison of reference and hybrid vehicle characteristics.

	Conventional	Pre-Transmission Parallel Hybrid
Vehicle Characteristics	Mass=1100 kg FRONTAL AREA=1.5 M^2 Coefficient of Drag=0.2	Mass=1297 kg FRONTAL AREA=1.5 M^2 Coefficient of Drag=0.2
Engine	1.7L CIDI Mercedes Benz (75 kW)	1.7L CIDI Mercedes Benz (75 kW)
Motor		UQM Permanent magnet (32 kW continuous)
Transmission	4 gear automatic (3:1, 1.7:1, 1:1, 0.7:1)	Modified Nissan CVT (ratio range 0.5 to 2.5)
Final drive	3.24:1	3.1:1
Battery	12v Pb-Acid (SLI)	Li-Ion 14Ah 96 elements ANL prototype
Accessories	Mechanical=500W Electrical=200W	Mechanical=500W Electrical=700W

t t

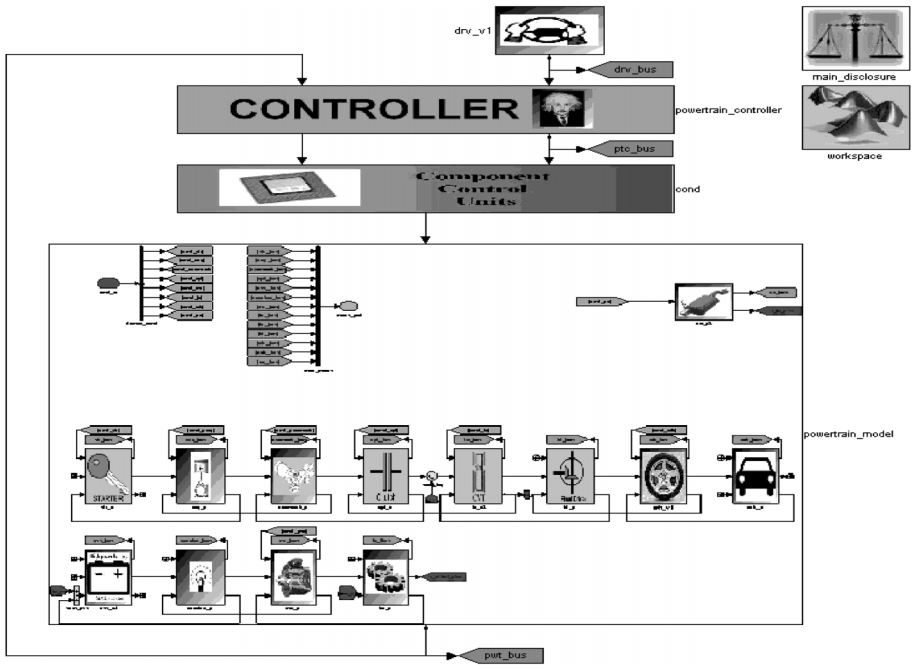

Figure 1. PSAT model–pre-transmission CVT parallel hybrid.

ransmission parallel hybrid powertrain used in this study.

2. COMPARISON OF CONTROL STRATEGIES

The philosophy behind the control strategies is that the energy in the system should be managed such that:

(1) Driver inputs (from brake and accelerating pedals) are satisfied consistently (driving the hybrid vehicle should not "feel" different from driving a conventional vehicle);

(2) The battery is sufficiently charged (to meet performance requirements); and

(3) The overall system efficiency is optimal (based on he engine, motor, battery, and transmission).

The power controller implements this philosophy (in the form of control rules or adaptive strategies) to determine how much power is needed to drive the wheels, how much to charge the battery and the power demand allocated to the engine and motor. If the battery needs to be charged, negative power is assigned to the electric motor, and the engine provides the power for both driving and charging the battery. To determine the optimal power split and the power generation/conversion of the individual components, efficiency maps of the components are used. Rule based and fuzzy logic strategies,

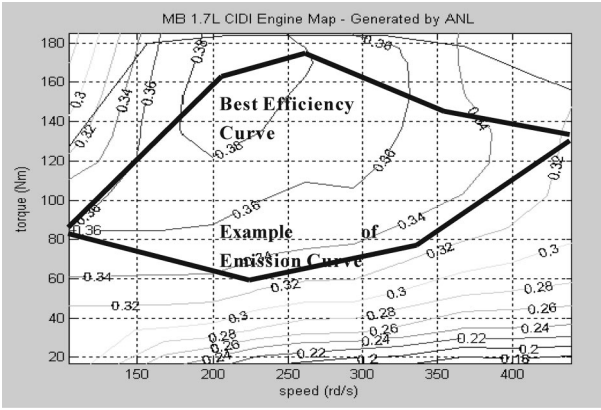

Figure 2. MB 1.7L Engine Map (ANL data).

described in the following paragraphs, were developed, simulated and compared in this paper.

2.1. Rule Based Control

Rule based control attempts to optimize engine efficiency by staying on the best efficiency curve. The engine can provide the required wheel power plus, depending upon state-of-charge (SOC), power to recharge the battery. Engine speed is regulated by the CVT ratio and the electric motor provides power to improve the overall drivetrain efficiency (e.g., used alone at low vehicle power demands).

2.2. Fuzzy Logic Control

The CIDI engine efficiency is highest for engine speeds between 180 and 260 rd/s on the optimal curve, corresponding to an engine power between 25 and 50 kW, with the absolute optimum at 44 kW. Therefore, the power-split strategy should preferably result in an engine power in this range. A similar approach has been used to analyze the efficiency of the permanent magnet motor/generator, however motor speed is directly related to vehicle speed and the efficiency can only be optimized by optimizing motor power at a given motor speed.

To study the trade-off between fuel economy and emissions, two strategies were tuned and analyzed:

(1) Fuel economy optimization (cf. Figure 2 upper curve);

(2) NOx emissions optimization (cf. Figure 2 lower curve).

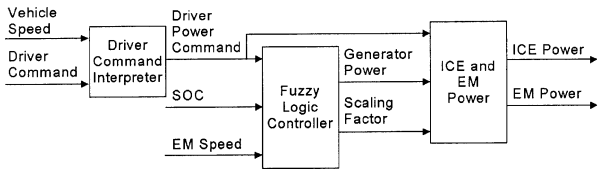

Figure 3. Fuzzy logic controller block diagram.

Table 2. Example rules of the fuzzy logic controller.

1	**If** SOC is too high **then** P_{gen} is 0 kW
2	**If** SOC is normal **and** P_{driver} is normal **and** ω is optimal **then** P_{gen} is 10 kW
3	**If** SOC is normal **and** ω_{EM} is **not** optimal **then** P_{gen} is 0 kW
4	**If** SOC is low **and** P_{driver} is normal **and** ω_{EM} is low **then** P_{gen} is 5 kW
5	**If** SOC is low **and** P_{driver} is normal **and** ω_{EM} is **not** low **then** P_{gen} is 15 kW
6	**If** SOC is too low **then** P_{gen} is $P_{gen,max}$
7	**If** SOC is too low **then** scale factor is 0
8	**If** SOC is **not** too low **and** P_{driver} is high **then** P_{gen} is 0 kW
9	**If** SOC is **not** too low **then** scale factor is 1

Figure 3 presents a simplified overview of the power controller. The first block converts the driver inputs from the brake and accelerator pedals to a driver power command. The signals from the pedals are normalized to a value between zero and one (zero: pedal is not pressed, one: pedal fully pressed). The braking pedal signal is then subtracted from the accelerating pedal signal, so that the driver input takes a value between –1 and +1.

The fuzzy energy management strategy described below has been implemented using a Takagi-Sugeno fuzzy logic controller (Takagi and Sugeno, 1985). A fuzzy logic controller relates the controller outputs to the inputs using a list of if-then statements called rules (example in Table 2). The if-part of the rules refers to adjectives that describe regions (fuzzy sets) of the input variable. A particular input value belongs to these regions to a certain

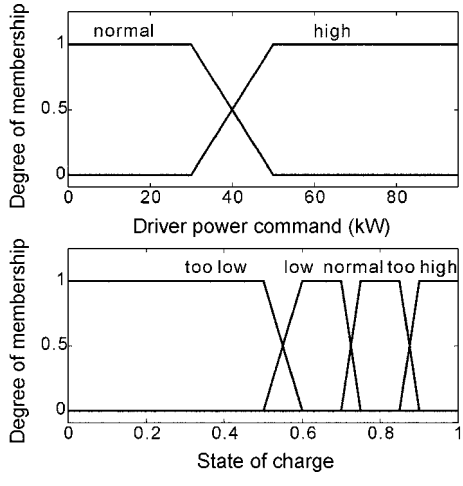

Figure 4. Example of membership functions.

degree, represented by the degree of membership (see Figure 4 for examples of membership functions that define the degree of membership). The then-part of the rules of a Takagi-Sugeno controller refers to values of the output variable. To obtain the output of the controller, the degrees of membership of the if-parts of all rules are evaluated, and the then-parts of all rules are averaged, weighted by these degrees of membership.

If the SOC is too high (rule 1) the desired generator power (Pgen) will be zero, to prevent overcharging the battery. If the SOC is normal (rules 2 and 3), the battery will only be charged when both the EM speed is optimal and the driver power is normal. If the SOC drops too low, the battery will be charged at a higher power level. This will result in a relatively fast recovery to a normal SOC. If the SOC drops to too low (rules 6 and 7), the SOC is increased as fast as possible to prevent battery damage. To achieve this, the generator power is maximized and the scaling factor is decreased from one to zero. Rule 8 prevents battery charging when the driver power demand is high and the SOC is not too low. Charging in this situation moves the engine power outside the optimum range (25-50 kW). Finally, when the SOC is not too low (rule 9), the scaling factor is one.

3. COMPARISON OF ENGINE MODELS

3.1. Neural Network

Neural network (NN) models were generated to simulate the transient behavior of fuel rate and NOx using a Pierburg Emissions Bench. The models were trained using selected transient data inputs recorded from a Mercedes 1.7L CIDI engine. The resultant neural network was validated using unique transient data recorded from the same engine.

3.2. Steady State Engine Map

To further quantify the simulation accuracy of the trained fuel rate NN model, an engine map (EM) model was generated using a locus of steady state operating point data recorded from the same engine. The model was instructed to simulate the same transient training and validation cycles previously submitted to the neural network model for simulation. Equivalent error plots and statistical error calculations were generated from the subsequent EM model simulation data results. The simulation accuracy of a NN model was then compared to the accuracy of the steady state EM model. The results are summarized in the following paragraph and details of the model generation and validation are included in the Appendix.

Figures 5 and 6 illustrate the differences in using fuel rate neural network and engine map models on the US06 validation cycle. The NN model simulation output was

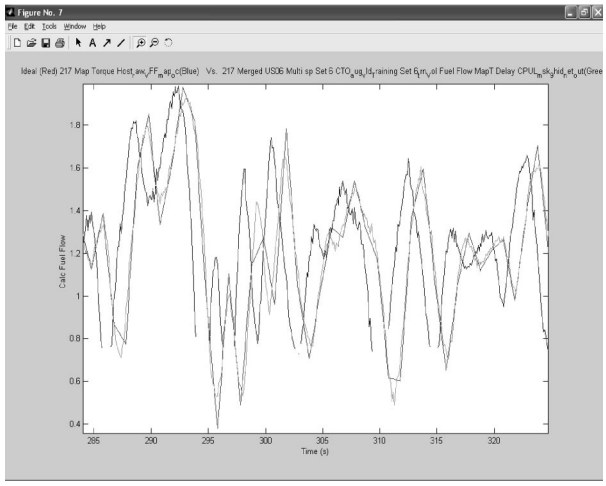

Figure 5. NN vs. EM model validation cycle (ANL data - red, EM - blue, NN - green).

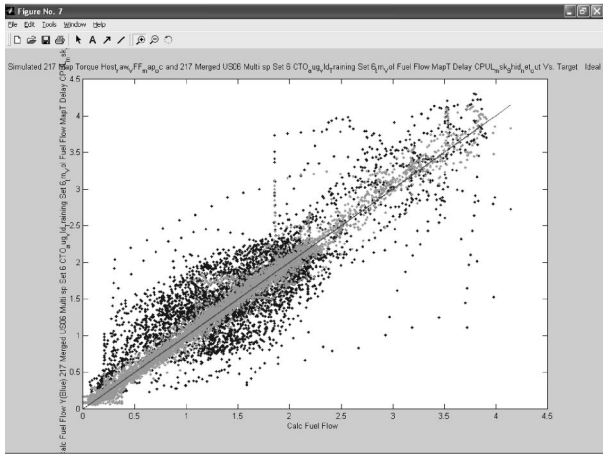

Figure 6. EM simulation vs. measured US06 data (ANL data - red, EM - blue, NN - green).

continuous and maintained minimal phase differential compared to the measured data. By contrast, the EM model simulation output contained magnitude errors and multiple discontinuities in addition to a time shift error with respect to the measured data. The EM model discontinuities are due to transient operation outside the bounds of the steady state data range, upon which the map model is predicated. The phase shift is likely due to measurement time delays in the test cell. Since the EM model is generated on mean steady state data, simulations using this model incorporate no time delay, and subsequently lead the measured data in time. The NN model not only simulated the volumetric fuel rate with accurate magnitude predictions, but also matched the phasing of the fuel rate data vector.

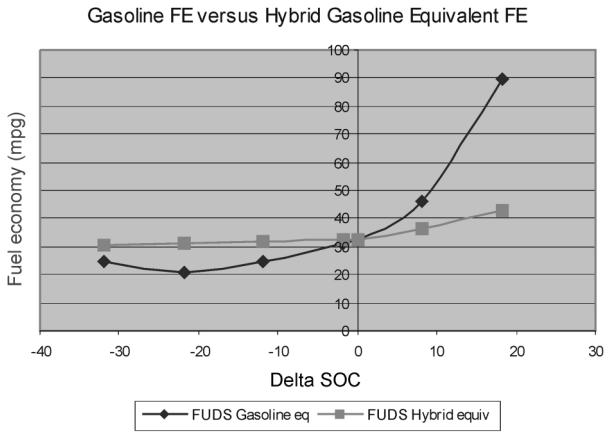

Figure 7. Fuel economy correction for SOC.

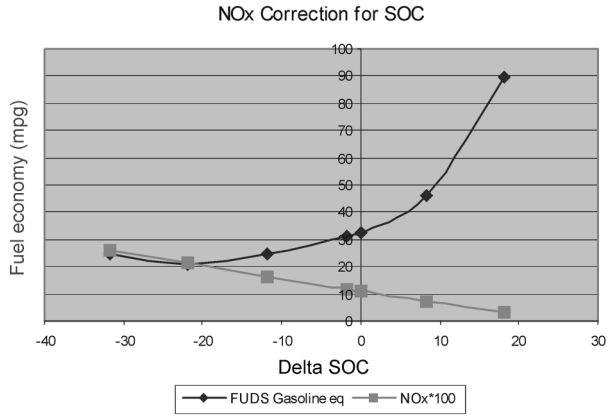

Figure 8. NOx correction for SOC.

4. RESULTS

The vehicle was simulated on urban and highway driving cycles using the two control strategies (rule based and fuzzy logic) and the neural network model (based on the previous comparison). Fuel economy and NOx emissions were compared taking into account battery SOC. Due to the significant impact of SOC on fuel economy and emissions, the method used in this study is presented first.

4.1. Influence of SOC on Fuel Economy and NOx Emissions

Initial and final SOC of the electrical energy storage device must be considered to accurately account for the total energy used when evaluating hybrid vehicle fuel economy. Either the initial SOC must equal the final SOC or a correction must be made. Figure 7, based on the following calculations, graphically illustrates the strong relationship between SOC difference and fuel economy (i.e., measured/estimated gasoline equivalent versus hybrid gasoline equivalent):

$$FEgasoline\_equivalent = \frac{Dis\tan ce(miles)}{Eq\_gal\_of\_gasoline}$$

$$Eq\_gal\_of\_gasoline = \frac{fuel\_heating\_value}{gasoline\_fuel\_heating\_value} \times fuel\_consum.(kg) \times \frac{liters2gal \times 1000}{fuel\_density}$$

$$FE\_hybrid\_gasoline\_eq = \frac{Dis\tan ce(miles)}{Eq\_gal\_of\_gasoline + Wh\_cons/Wh\_per\_gal/Battery\_eff/Charg\_eff/Engineering}$$

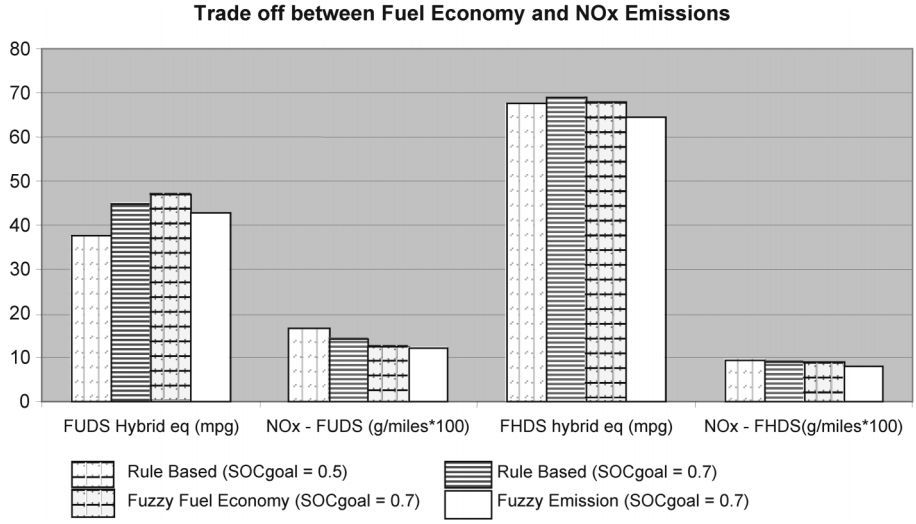

Figure 9. Influence of control strategy on fuel economy and NOx emissions.

The hybrid gasoline equivalent fuel economy estimates the energy necessary to recharge the battery to its initial SOC. The figure shows comparable values when initial and final SOC are close, but differences can be significant as the difference increases. Using the same methodology, Figure 8 demonstrates that NOx emissions can also be SOC corrected.

4.2. Influence of Control Strategy on Fuel Economy and NOx Emissions

Figure 9 illustrates the impact of SOC and control strategy on fuel economy and NOx emissions:

(1) SOC significantly affects the results on the urban cycle; for rule based control, changing the SOC goal from 0.5 to 0.7 increases fuel economy by almost 20% as well as reduces NOx emissions;

(2) Fuzzy logic needs to be refined for the highway cycle since better results are obtained with rule based control;

(3) Variation of −/+ 10% in fuel economy and NOx emissions can be obtained by varying control strategy philosophy and parameters;

(4) In addition to control strategy, initial conditions and overall system efficiency induce a variation of fuel economy and NOx results.

When developing a control strategy, trade-offs other than fuel economy and emissions should be taken into account. For example, battery life considerations could dictate SOC lower than 0.7 even if fuel economy and NOx might be penalized.

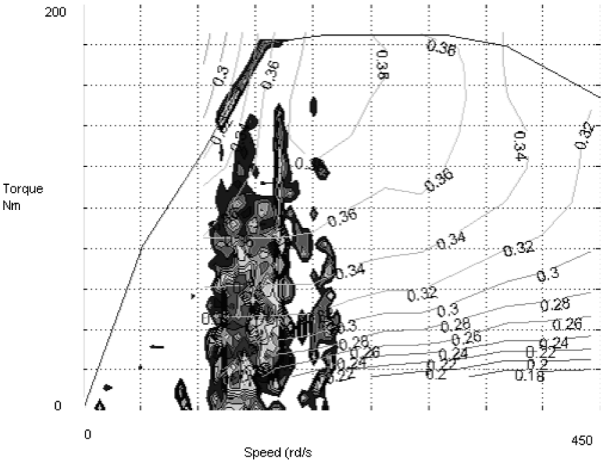

Figure 10. Operating points (conventional).

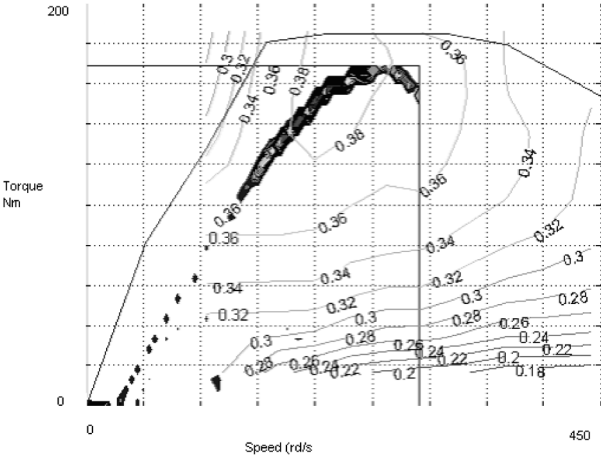

Figure 11. Operating points (hybrid).

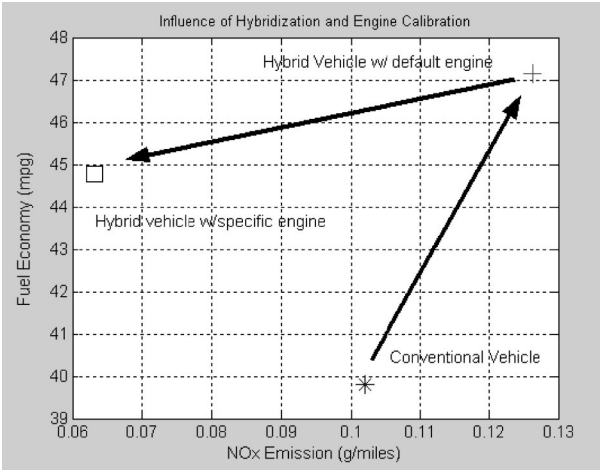

Figure 12. Trade-off between fuel economy and NOx emissions.

4.3. Influence of Hybridization on Fuel Economy and NOx Emissions

Hybridization can increase fuel economy by keeping the engine in an optimum efficiency range. In general, and in particular for the engine considered in this study, this means higher average load and speed which leads to higher average operating temperature and higher NOx emissions. The following figures compare the operating points for the same engine in conventional (Figure 10) and hybrid (Figure 11) vehicle applications to illustrate this point.

This comparison supports the results of the analysis in this study, illustrated in Figure 12, that hybridization without changing engine size can increase fuel economy (18% in the example), but increase NOx emissions (25% in the example). However, if the engine had ideal characteristics for a hybrid vehicle with larger islands of high efficiency and low emissions (originally developed for the PNGV program), the result could be a fuel economy increase of about 13% accompanied by a NOx decrease of almost 40%.

5. CONCLUSION

A neural network model was developed to realistically assess NOx emission. We demonstrated that hybridization allows both the diminution of both fuel consumption and NOx emission. Moreover, control strategies philosophies as well as parameter values also play an important part of the trade-off between fuel economy and emission. However, even if hybridization and control play an important role, optimizing the entire system remains the ultimate solution. To do so, each component has to be chosen and calibrated based on a system prospective. In order to validate the tools developed, control strategies will be integrated and tested on a bench with real component using Hardware-in-the-Loop.

ACKNOWLEDGMENTS–This work was supported by the U.S. Department of Energy, under contract W-31-109-Eng-38. The authors would like to thank Bob Kost and Pat Sutton from DOE who sponsor this activity. The authors would finally like to thank USCAR for their support and ANL test team for the useful data they provided.

REFERENCES

An, F. and Rousseau, A. (2001). Integration of a modal energy and emission model into the PNGV vehicle simulation model: PSAT. *SAE World Congress 2001*, Detroit, March 4-8.

Deville, B. and Rousseau, A. (2001). *Validation of the Honda Insight Using PSAT*. DOE Report. September 2001.

Karnopp, D., Margolis, D. and Rosenberg, R. (1990). *System Dynamics: A Unified Approach*. 2nd ed. John Wiley & Sons, Inc., New York.

Rousseau, A., Deville, B., Zini, G., Kern, J., Anderson, J. and Duoba, M. (2001). Honda insight validation using PSAT. Future Transportation Technology Conference, Costa-Mesa, *SAE Paper No. 01-2538*.

Rousseau, A. and Larsen, R. (2000). Simulation and validation of hybrid electric vehicles using PSAT. *Global Powertrain Congress*, Detroit, June 68.

Rousseau, A., Pagerit, S. and Monnet, G. (2001). The new PNGV system analysis toolkit PSAT V4.1 evolution and improvements. Future Transportation Technology Conference, Costa-Mesa, *SAE Paper No. 01-2536.*

Rousseau, A. and Pasquier, M. (2001). Validation of a hybrid modeling software (PSAT) using its extension for prototyping (PSAT-PRO). *Global Powertrain Congress*, Detroit, June 06-08.

Rousseau, A. and Pasquier, M. (2001). Validation process of a system analysis model: PSAT. *SAE Paper No. 01-P183*, SAE World Congress, Detroit, March 4-8.

Sharer, P. and Rousseau, A. (2001). *Validation of the Japan Toyota Prius Using PSAT*. DOE Report, March 2001.

Takagi, T. and Sugeno, M. (1985). Fuzzy identification of systems and its application to modeling and control. *IEEE Transactions on Systems*, Man and Cybernetics, **15, 1,** 116–132.

APPENDIX - Engine Model Development

Neural Network Model

Neural Network (NN) models were generated to simulate the transient behavior of fuel rate and NOx obtained from a Pierburg emissions bench. The Neural Network models were trained using selected transient data inputs recorded from a Mercedes 1.7L CIDI engine. The resultant neural network was validated using unique transient data recorded from the 1.7L CIDI engine.

Neural Network Training Data

Training data, recorded from transient operation of the 1.7L CIDI engine, was submitted to the NN models in contiguous block form. The training data consisted of a collection of (4) geometric transient cycles, and (3) drive cycles. The training data was selected to encompass the widest range of engine operation, first in simulated drive cycle operation, and second through augmentation of drive cycle data with geometric transient cycles. The combination of both transient cycle data topologies provided wide engine map coverage.

Neural Network Training

The training data was presented to the NN a series of times, and training was discontinued at the point of

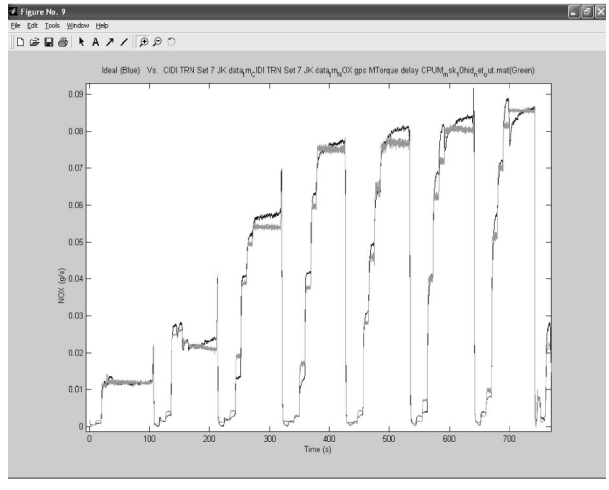

Figure A-1. NOx NN model validation (measured - blue, simulated - green).

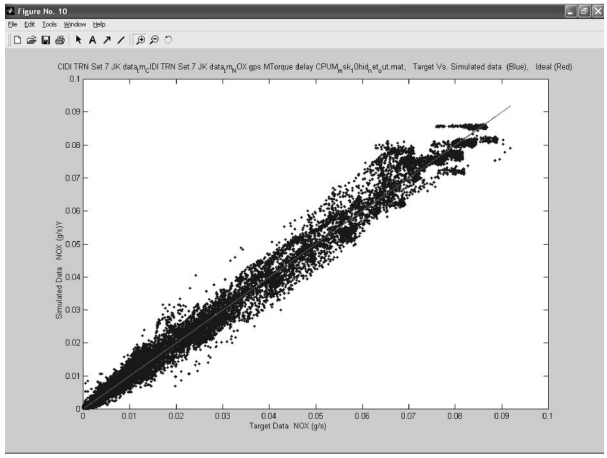

Figure A-2. NOx simulated vs. measured training data.

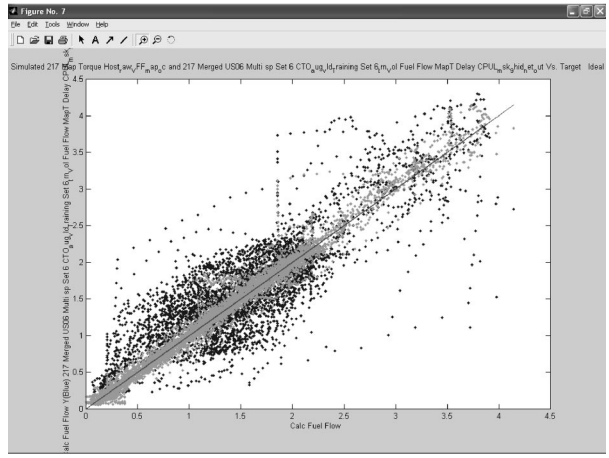

Figure A-4. EMM simulation vs. measured US06 data.

diminishing return. In particular, once the simulation error no longer decreased, following exposure to another training set session, the training session was terminated. The inputs to the NN model were engine speed, map torque and time delayed map torque. The fuel rate neural models incorporated a total of nine hidden neurons, in addition to the output fuel rate neuron, and the input vector neurons, whereas the NOx neural model has a total of ten hidden neurons, in addition to the output NOx neuron, and the input vector neurons.

Evaluation of Training Effectiveness

The trained NN model was presented with the training set data and instructed to simulate said data accordingly. Comparison of simulated vs. measured data was plotted against time, in addition to simulated data vs. measured data. Error calculations were performed; the quality of the simulation was defined by the error plots and forthcoming statistical error calculations. Figure X illustrates the simulation accuracy through comparison to the measured data. The simulation data is identified in green, and the measured data in blue.

Steady State Model

To further quantify the simulation accuracy of the trained fuel rate NN model, an engine map (EM) model was generated using a locus of steady state operating point data recorded from the same engine. The model was instructed to simulate the same transient training and validation cycles previously submitted to the neural network model for simulation. Equivalent error plots and statistical error calculations were generated from the

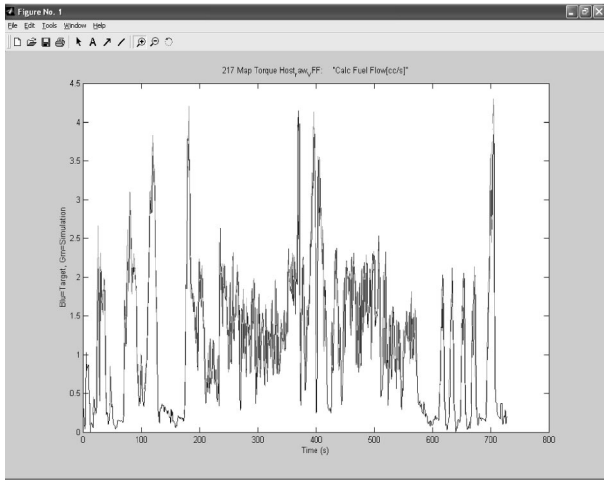

Figure A-3. US06 VFF EMM validation drive cycle (Measured data - blue, EM model simulation - green).

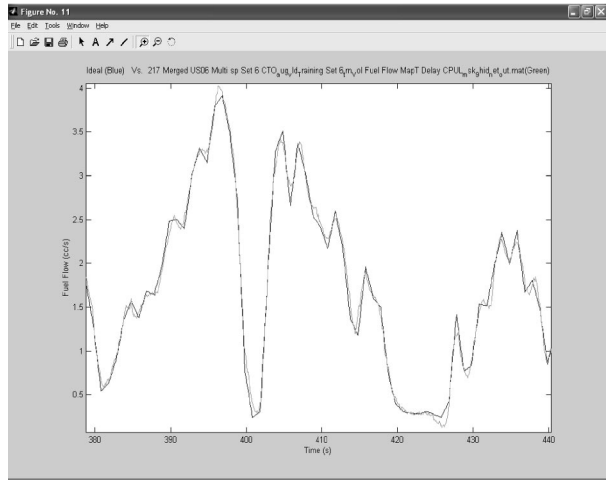

Figure A-5. Zoom plot US06 fuel rate NN validation US06.

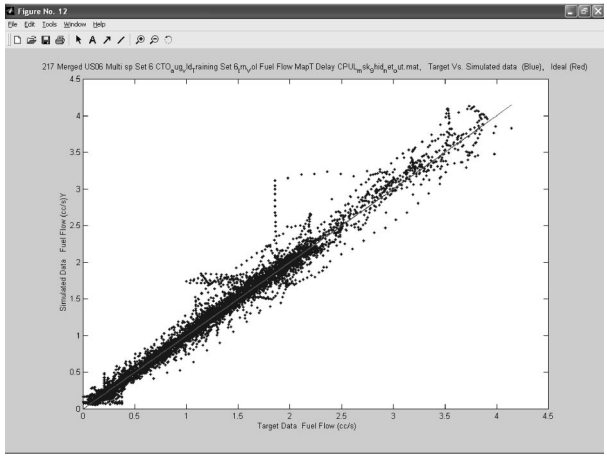

Figure A-6. Fuel rate simulated vs. measured.

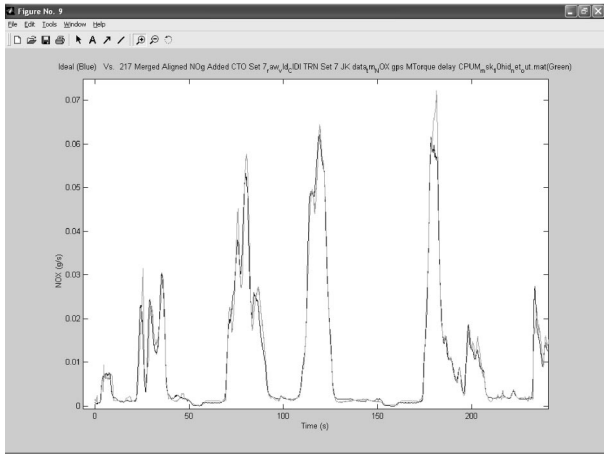

Figure A-7. Zoom plot US06 NOx NN validation.

subsequent EM model simulation data results. The simulation accuracy of a NN model was then compared

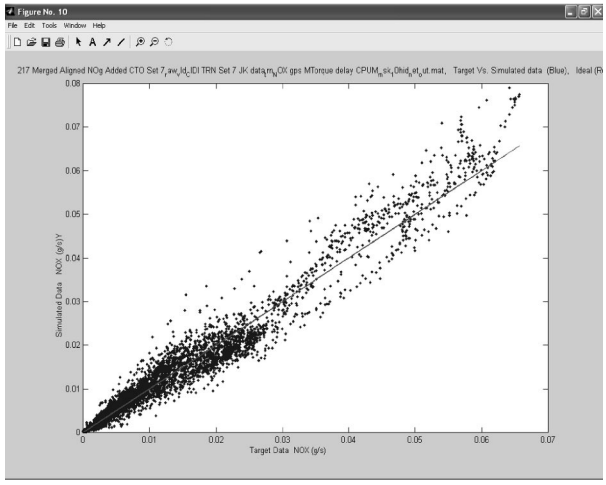

Figure A-8. NOx simulated vs. measured US06.

to the accuracy of the steady state EM model. Figures A-3 and A-4 show the NN model vs. EM model comparison using the US06 Validation cycle.

Validation of Neural Network Model using Transient Test Data

The trained NN model, having predicted the training data with a high degree of precision, was next evaluated with data never before introduced to this model. Each cycle was individually presented to the trained NN model, and subsequent comparison and error plots were generated. Error calculations revealed the simulation coefficient of determination (R^2) deviation from ideal was in the range of 0.9691 to 0.9946 for the fuel rate model and 0.8453 to 0.9947 for the Pierburg NOx model.

Figures A-5 through A-8 illustrate an example of the simulation of a US06 validation driving cycle using the volumetric fuel rate NN model as well as the Pierburg NOx NN model.